Adsorption 5, 359–368 (1999)

Binary Adsorption of Phenol and m-Cresol Mixtures onto a Polymeric Adsorbent

AGOSTINHO GARCIA, LICINIO FERREIRA, ANABELA LEITÃO AND ALÍRIO RODRIGUES
Laboratory of Separation and Reaction Engineering, School of Engineering, University of Porto, 4099 Porto Codex, Portugal

Received June 29, 1998; Revised January 21, 1999; Accepted April 2, 1999

Abstract. Adsorption processes are gaining interest as methods of purifying industrial effluents. Most industries discharge effluents containing several components. The adsorption of phenol and m-cresol mixtures from aqueous solutions onto a macroporous polymeric adsorbent, Duolite ES-861, was investigated experimentally in a fixed-bed adsorber for different flowrates, feed concentrations and bed initial conditions (clean or pre-saturated).

The experimental results are presented in this work, where the major objective is placed on the modelling of these fixed bed adsorption experiments using an extended Langmuir isotherm equation for two components, based on single component equilibrium data obtained for phenol and m-cresol.

The model presented in this paper takes into account axial dispersion of the liquid phase, film diffusion and intraparticle mass transfer and successfully simulates the adsorption behaviour of the phenol and m-cresol mixtures.

Keywords: binary adsorption, polymeric adsorbents, fixed bed adsorption

1. Introduction

Increasing concern for public health and environmental quality has lead to the establishment of limits on the acceptable environmental levels of specific pollutants. Polynuclear aromatic hydrocarbons (PAH) and phenolic compounds are two classes of compounds widely prevalent in the environment and classified by EPA as priority pollutants. Naphthalene and substituted naphthalenes, the simplest members of PAH, have a greater tendency to migrate from petroleum oils into the marine environment and contaminate industrial water (Grunfeld and Frank, 1977). Phenolic compounds, entering the aquatic environment through direct discharge from coke ovens in steel plants, refineries, pulp and paper industries, etc, impart objectionable taste and odor to drinking water at concentrations as low as 0.005 mg/l. Consequently, there has been a growing interest in developing processes of removing these compounds from water. Adsorption is often the preferred separation process since it can be used for removing a variety of organics from aqueous systems (Gusler et al., 1993; McKay and Al-Duri, 1988; Moon et al., 1991; Calleja et al., 1993).

Adsorption of phenolic compounds onto microporous activated carbon is of great interest due to the high adsorption capacity of this adsorbent (Calleja et al., 1993). However, the regeneration of spent carbon is not easy because of considerable irreversible adsorption (Costa and Rodrigues, 1985a). Since regeneration efficiency is a critical factor for the economy of the overall adsorption process, polymeric adsorbents are used as an alternative to activated carbon for the removal of organic substances from aqueous solutions (Costa and Rodrigues, 1985a, 1985b; Garcia and King, 1989; Rixey and King, 1989). The regeneration of these adsorbents is accomplished by leaching with alkaline solutions (Costa and Rodrigues, 1985a, 1985b). Adsorption calculations for the design of a cyclic process require information on adsorption equilibria, intraparticle mass transfer of adsorbates and regeneration. Multicomponent equilibrium data are tedious to obtain

experimentally and a lot of effort has been made to predict multicomponent equilibrium data based on only single component isotherm data (Myers and Prausnitz, 1965; Suwanayuen and Danner, 1980; Reich et al., 1980).

The present work is concerned with the adsorption of phenol and m-cresol mixtures onto a Duolite ES-861 resin. The major objective of this work is placed on the modelling of fixed bed adsorption experiments using an extended Langmuir isotherm equation for two components based on single component equilibrium data.

2. Experimental

The adsorbent used in this study is a macroporous polymeric adsorbent (Duolite ES861, Rohm and Haas). The adsorbent is based on a polystyrene matrix crosslinked with divinylbenzene and has properties summarised in Table 1. The adsorbates are phenol and m-cresol. Binary solutions were prepared by dissolving the reagent-grade chemicals supplied by Merck into distilled and deionized water.

Table 1. Properties of the Duolite ES-861 resin.

Wet density—ρ_h (g wet resin/l resin)	1020
Apparent density—ρ_a (g dry resin/l resin)	285.6
Real density—ρ_r (g dry resin/l polymer)	1040
BET surface area (m^2/g)	500
Particle porosity—ε_p	0.72
Particle diameter—d_p (mm)	0.47

Adsorption experiments were conducted in a fixed-bed adsorber of 39 cm length and 2.18 cm diameter packed with the resin particles. All the experiments were carried out at 20°C, by using different flowrates up to 115 ml/min, feed concentrations up to around 200 mg/l and bed initial conditions (clean or presaturated) as depicted in Table 2.

The concentrations of phenol and m-cresol in the liquid at the outlet of the column in response to a step input of these species concentrations were determined by using a VARIAN AEROGRAPH 1400 gas chromatograph, with FID detection and a 1829×2 mm glass column packed with 0.1% SP-1000 in Carbopack C. The column temperature was set at 225°C and the carrier gas was nitrogen at 20 ml/min.

3. Adsorption Isotherm

Single solute adsorption equilibrium data for phenol and m-cresol onto DUOLITE ES-861 were obtained by Ramalho (1993) and were represented by Langmuir isotherms.

In the present work the multicomponent adsorption equilibrium is predicted by the extended Langmuir equation:

$$q_i^* = \frac{K_{Li} Q_L C_i^*}{1 + \sum_{i=1}^{2} K_{Li} C_i^*} \tag{1}$$

where q_i^* is the adsorbed concentration of component i in equilibrium with the liquid concentration

Table 2. Experimental conditions for fixed bed adsorption.

Run	U (ml/min)	u_0 (cm/min)	ε	τ (min)	C_{f1} (mg/l)	C_{f2} (mg/l)	C_{01} (mg/l)	C_{02} (mg/l)
1	40	10.78	0.42	1.52	118		0	0
2	51	13.54	0.42	1.21		100	0	0
3	41	10.99	0.42	1.49	100	88	0	0
4	115	30.91	0.42	0.53	96	93	0	0
5	43	11.54	0.42	1.42	60	156	0	0
6	47	12.50	0.42	1.31	158	49	0	0
7	13	3.50	0.42	4.68	112	93	0	0
8	48	13.00	0.42	1.26	104	98	0	0
9	43	11.54	0.42	1.42	175	18	0	0
10	47	12.50	0.42	1.31	108	102	0	0
11	51	13.54	0.42	1.21	0	204	100	104
12	43	11.54	0.42	1.42	214	0	108	102
13	47	12.50	0.42	1.31	0	188	185	13

C_i^*. The isotherm parameters $Q_L = 141.0$ mg/g, $K_{L1} = 0.0017$ l/mg and $K_{L2} = 0.0065$ l/mg were estimated from the single component equilibrium data. Calculated isotherms by using Eq. (1) are shown in Fig. 1(a) and (b) for phenol and m-cresol, respectively.

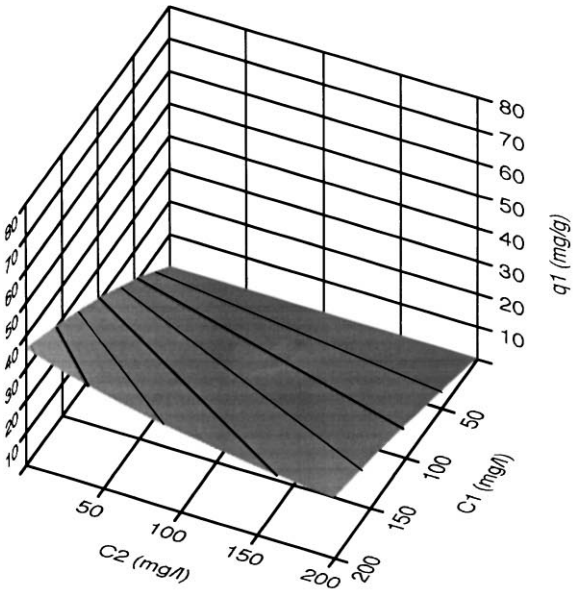

(a)

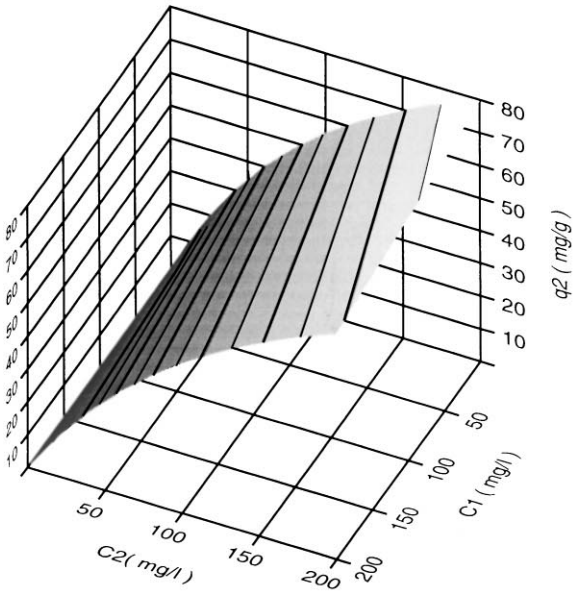

(b)

Figure 1. Multicomponent adsorption isotherm: (a) phenol; (b) m-cresol.

4. Mathematical Model for Fixed Bed Adsorption

4.1. Model Equations

Based on the assumptions: (a) intraparticle mass transfer takes place by diffusion in the liquid phase filling the pores; (b) the effective diffusivities are taken to be constant; (c) the equilibrium of adsorption is instantaneously achieved at the pore/wall interface; (d) the adsorbent particles are spherical; (e) the hydrodynamics of the bed fluid is described by the dispersed plug-flow model; the following dimensionless mass balance equations, with respective initial and boundary conditions, may be written for the species m ($m = 1, 2$):

(a) Bed fluid

$$\frac{\partial X_m(z^*,\theta)}{\partial \theta} = \frac{1}{Pe}\frac{\partial^2 X_m(z^*,\theta)}{\partial z^{*2}} - \frac{\partial X_m(z^*,\theta)}{\partial z^*} - N_{fm}(X_m(z^*,\theta) - X_{pm}(1,z^*,\theta)) \tag{2}$$

—Initial conditions

$$X_m(z^*,0) = X_{0m} \tag{3}$$

—Boundary conditions

$$X_m(0,\theta) = 1 \tag{4}$$

$$\left.\frac{\partial X_m(z^*,\theta)}{\partial z^*}\right|_{z^*=1} = 0 \tag{5}$$

(b) Particle

$$\frac{\partial y_m(u^*,z^*,\theta)}{\partial \theta} = N_{dm}\left(\frac{\partial^2 X_{pm}(u^*,z^*,\theta)}{\partial u^{*2}} + \frac{2}{u^*}\frac{\partial X_{pm}(u^*,z^*,\theta)}{\partial u^*}\right) \tag{6}$$

with

$$y_m = \varepsilon_p X_{pm} + \frac{\rho_a K_{Lm} Q_L X_{pm}}{1 + K_{L1}C_{f1}X_{p1} + K_{L2}C_{f2}X_{p2}} \tag{7}$$

—Initial conditions

$$X_{pm}(u^*,z^*,0) = X_{0m} \tag{8}$$

—Boundary conditions

$$\left.\frac{\partial X_{pm}(u^*, z^*, \theta)}{\partial u^*}\right|_{u^*=0} = 0 \tag{9}$$

$$N_{fm}(X_m(z^*, \theta) - X_{pm}(1, z^*, \theta)) = 3\frac{1-\varepsilon}{\varepsilon} N_{dm} \left.\frac{\partial X_{pm}(u^*, z^*, \theta)}{\partial u^*}\right|_{u^*=1} \tag{10}$$

In the above equations $X_m = C_m/C_{fm}$ and $X_{pm} = C_{pm}/C_{fm}$ are the dimensionless concentrations of the species m in the bulk liquid phase and in the liquid inside particle pores, respectively; y_m is the total (liquid + adsorbed) concentration of the species m inside particles; $\theta = t/\tau$ is a reduced time (τ is the bed space time); $X_{0m} = C_{0m}/C_{fm}$ is the dimensionless liquid concentration of the species m inside the column at initial time (0 for a clean bed or $\neq 0$ for a presaturated bed); $N_{dm} = \tau D_{pm}\varepsilon_p/R^2$ is the number of mass transfer units for species m pore diffusion ($D_{pm} = D_{mm}/\tau_p$ is the species m effective diffusivity and τ_p is the resin tortuosity factor); $N_{fm} = 3\frac{1-\varepsilon}{\varepsilon}\frac{K_{fm}\tau}{R}$ is the number of mass transfer units for species m external film diffusion (K_{fm} is the film mass transfer coefficient for species m) and $Pe = u_i L/D_{ax}$ is axial Peclet number (D_{ax} is the axial dispersion coefficient).

4.2. Numerical Solution

Model equations, Eqs. (2)–(10), were solved by using the following numerical technique:

a) First, the mass balance for the two components inside particles, expressed as:

$$\frac{\partial X_{p1}}{\partial \theta} = \frac{c_2}{b_1c_2 - b_2c_1} N_{d1}\left(\frac{\partial^2 X_{p1}}{\partial u^{*2}} + \frac{2}{u^*}\frac{\partial X_{p1}}{\partial u^*}\right) - \frac{b_2}{b_1c_2 - b_2c_1} N_{d2}\left(\frac{\partial^2 X_{p2}}{\partial u^{*2}} + \frac{2}{u^*}\frac{\partial X_{p2}}{\partial u^*}\right) \tag{11}$$

$$\frac{\partial X_{p2}}{\partial \theta} = \frac{b_1}{b_1c_2 - b_2c_1} N_{d2}\left(\frac{\partial^2 X_{p2}}{\partial u^{*2}} + \frac{2}{u^*}\frac{\partial X_{p2}}{\partial u^*}\right) - \frac{c_1}{b_1c_2 - b_2c_1} N_{d1}\left(\frac{\partial^2 X_{p1}}{\partial u^{*2}} + \frac{2}{u^*}\frac{\partial X_{p1}}{\partial u^*}\right) \tag{12}$$

with

$$b_1 = \frac{\partial y_1}{\partial X_{p1}} = \varepsilon_p + \frac{\rho_a K_{L1} Q_L (1 + K_{L2}C_{f2}X_{p2})}{(1 + K_{L1}C_{f1}X_{p1} + K_{L2}C_{f2}X_{p2})^2} \tag{13}$$

$$b_2 = \frac{\partial y_1}{\partial X_{p2}} = -\frac{\rho_a K_{L1} K_{L2} Q_L C_{f2} X_{p1}}{(1 + K_{L1}C_{f1}X_{p1} + K_{L2}C_{f2}X_{p2})^2} \tag{14}$$

$$c_1 = \frac{\partial y_2}{\partial X_{p1}} = -\frac{\rho_a K_{L1} K_{L2} Q_L C_{f1} X_{p2}}{(1 + K_{L1}C_{f1}X_{p1} + K_{L2}C_{f2}X_{p2})^2} \tag{15}$$

$$c_2 = \frac{\partial y_2}{\partial X_{p2}} = \varepsilon_p + \frac{\rho_a K_{L2} Q_L (1 + K_{L1}C_{f1}X_{p1})}{(1 + K_{L1}C_{f1}X_{p1} + K_{L2}C_{f2}X_{p2})^2} \tag{16}$$

including their initial and boundary conditions, were discretized along the particle radial coordinate, u^*, by using orthogonal collocation on finite elements with cubic Hermite polynomials as basis functions (Finlayson, 1980). The interval $0 \le u^* \le 1$ was divided into NE subintervals, with two collocation points within each subinterval. The solutions X_{p1} and X_{p2} in the kth subinterval of u^* were approximated by:

$$X_{p1}(g_j, z^*\theta) = \sum_{i=1}^{4} a^1_{i+2k-2}(z^*, \theta) H_{ji} \tag{17}$$

$$X_{p2}(g_j, z^*\theta) = \sum_{i=1}^{4} a^2_{i+2k-2}(z^*, \theta) H_{ji} \tag{18}$$

where g_j, with $j = 1, 2$, are the collocation points within each subinterval of u^*. After the discretization process, we obtained a system of $2 \times 2NE = 4NE$ partial differential equations in the basis function coefficients a_1's and a_2's dependent on the bed axial coordinate, z^*, and time, θ.

b) Second, the system of PDE's composed by the $4NE$ equations resulting from the discretization step and the mass balance equations in the bulk fluid phase, Eqs. (2) with $m = 1, 2$, was numerically integrated with the PDECOL package (Madsen and Sincovec, 1979).

Table 3. Values for the model parameters.

Run	1	2	3	4	5	6	7	8	9	10	11	12	13
Pe	120	120	120	120	120	120	120	120	120	120	120	120	120
N_{d1}	0.75	—	0.74	0.26	0.71	0.65	2.33	0.63	0.71	0.65	0.60	0.71	0.65
N_{d2}	—	0.57	0.70	0.25	0.67	0.62	2.20	0.59	0.67	0.62	0.57	0.67	0.62
N_{f1}	157.8	—	156.1	86.7	152.2	145.2	299.6	142.0	152.2	145.2	139.0	152.2	145.2
N_{f2}	—	133.7	150.2	83.3	146.5	139.7	288.2	136.6	146.5	139.7	133.7	146.5	139.7

5. Results and Discussion

Model equations were solved for the adsorption of phenol and m-cresol and the solution, in terms of the concentrations of these species at column outlet as a function of time time, was compared with experimental data.

Table 3 shows the values taken for the model parameters in each experiment. The bed axial Peclet number, *Pe*, was determined from tracer experiments (Ferreira, 1994). The film mass transfer coefficients for phenol and m-cresol, K_{f1} and K_{f2}, were calculated by using the correlation:

$$j_D = 7.32 Re'^{(-0.567)} \tag{19}$$

where

$$Re' = \frac{u_0 d_p}{\nu(1-\varepsilon)}; \quad j_D = \frac{Sh}{Re'(1-\varepsilon)Sc^{1/3}};$$

$$Sh = \frac{K_f d_p}{D_m}; \quad Sc = \frac{\nu}{D_m}$$

The molecular diffusivities of phenol and m-cresol, D_{m1} and D_{m2}, in aqueous solutions at 20°C, were estimated by the Wilke-Chang equation, as being 8.9×10^{-6} and 8.4×10^{-6} cm^2/s (Ramalho, 1993), respectively.

5.1. Single Component Experiments

Figure 2(a) and (b) show the monocomponent breakthrough curves for phenol (run 1) and m-cresol (run 2), respectively. The stoichiometric time is clearly higher for m-cresol due to the higher affinity of the resin for this component. The model was fitted to the experimental outlet concentration data obtained for phenol by using the number of mass transfer units for phenol pore diffusion, N_{d1}, as an adjustable parameter. From

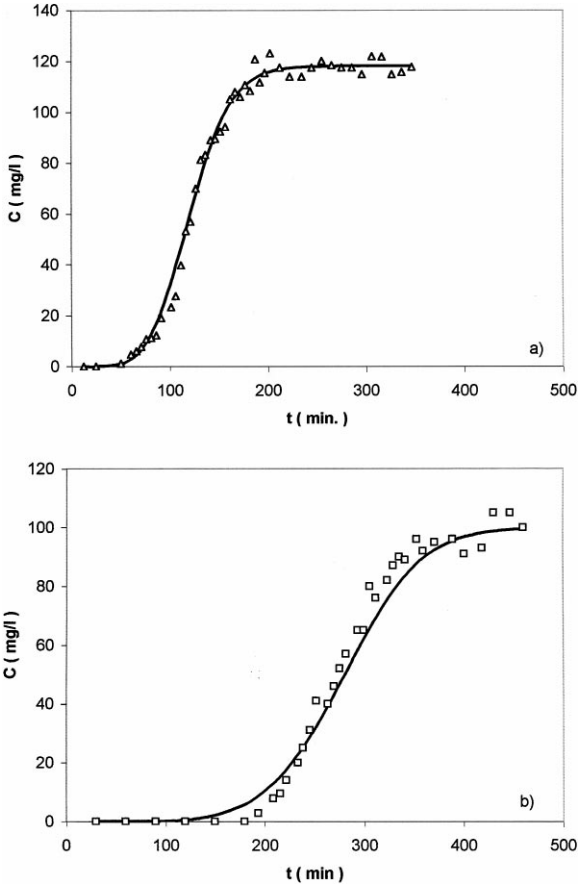

Figure 2. Fixed-bed breakthrough curves for single components: (a) phenol (△△△); (b) m-cresol (□□□).

the best value found for N_{d1}(=0.75), the value for the resin tortuosity factor was obtained as being 1.4. This value is in close agreement with predictions of the tortuosity factor according to the spherical-cell pore model of Weisz and Schwartz (1962),

$$\tau_p = \sqrt{3}/(1.5\varepsilon_p) = 1.60$$

or according to the random-pore model of Wakao and Smith (1962),

$$\tau_p = 1/\varepsilon_p = 1.39$$

In Fig. 2(b) the breakthrough curve for m-cresol was calculated with a value for $N_{d2} = 0.57$, determined by using the previously found resin tortuosity factor. The calculated and experimental breakthrough curves are not in so close agreement as for phenol. For m-cresol a higher N_d value is needed for a better fitting, leading to a tortuosity factor close to 1, which suggests that m-cresol surface diffusion should be considered in the mathematical model, probably due to the higher slope of the Langmuir adsorption isotherm for this component.

5.2. Multicomponent Experiments

5.2.1. Effects of the Flowrate, Feed Concentrations and Bed Initial Conditions. Figures 3–5 show the bed outlet concentration curves, when binary mixtures of phenol and m-cresol are fed to the column, illustrating the effects of the flowrate, feed concentrations and bed initial conditions. The concentration curves were calculated by using the equilibrium data expressed by Eq. (1), with parameters estimated from the single component isotherms, and the N_d values for phenol and m-cresol listed in Table 3, which were obtained with the resin tortuosity factor equal to 1.4. A reasonable agreement is observed between experimental and calculated concentration curves in all experiments, validating the simple method used in our work to predict the multicomponent adsorption equilibrium.

Figures 3(a)–(c) illustrate that the phenol and m-cresol breakthrough curves become closer as the flowrate increases due to the lower number of mass transfer units for pore diffusion. At low flowrates operating conditions are closer to equilibrium and the intermediate plateau is clearly observed. In all cases roll-up phenomenon of the less adsorbed component occurs.

Figures 4(a)–(d) illustrate that the less adsorbed component, phenol, is always displaced by the more adsorbed component, m-cresol. Various feed compositions were considered ranging from phenol rich feed (4c) to m-cresol rich feed (4b).

In Fig. 5(b)–(d) the fixed-bed was initially presaturated with a given binary mixture of phenol and m-cresol before feeding the new mixture. The results in Fig. 6 show that the pore diffusion model (dashed lines)

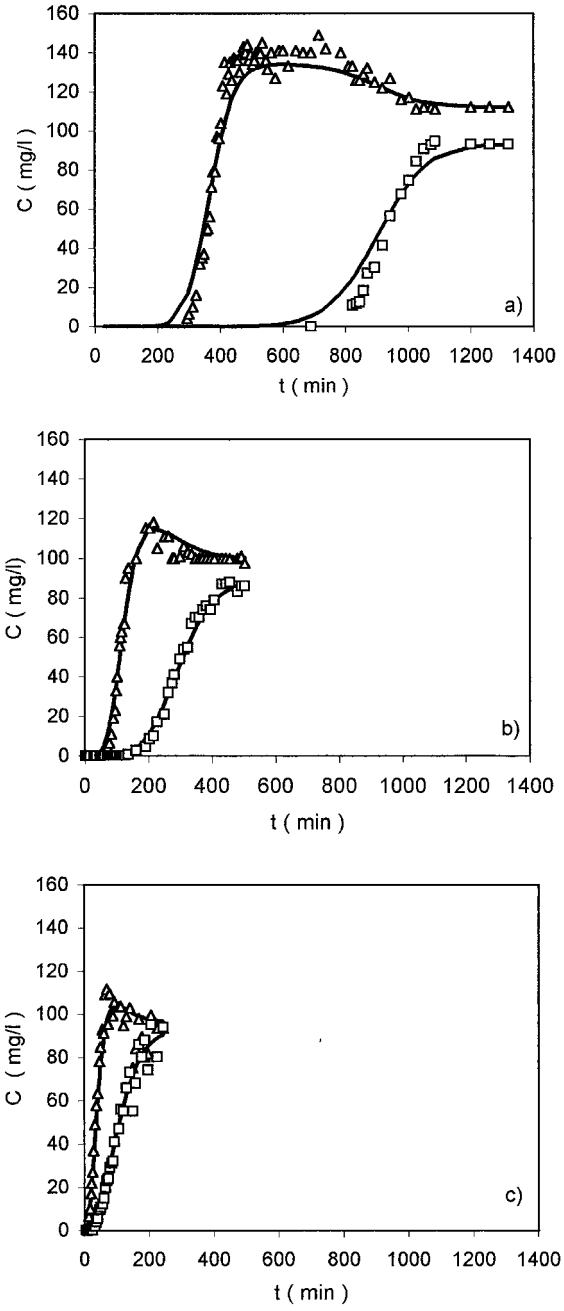

Figure 3. Effect of the flowrate on breakthrough curves for binary mixtures of phenol (△△△) and m-cresol (□□□) fed to the column: (a) $U = 13$ ml/min (run 7); (b) $U = 41$ ml/min (run 3); (c) $U = 115$ ml/min (run 4).

represents more adequately the experimental data than the model where diffusional resistances are not considered, equilibrium model (solid lines). The displacement of phenol by m-cresol in Fig. 6(a) and of m-cresol by

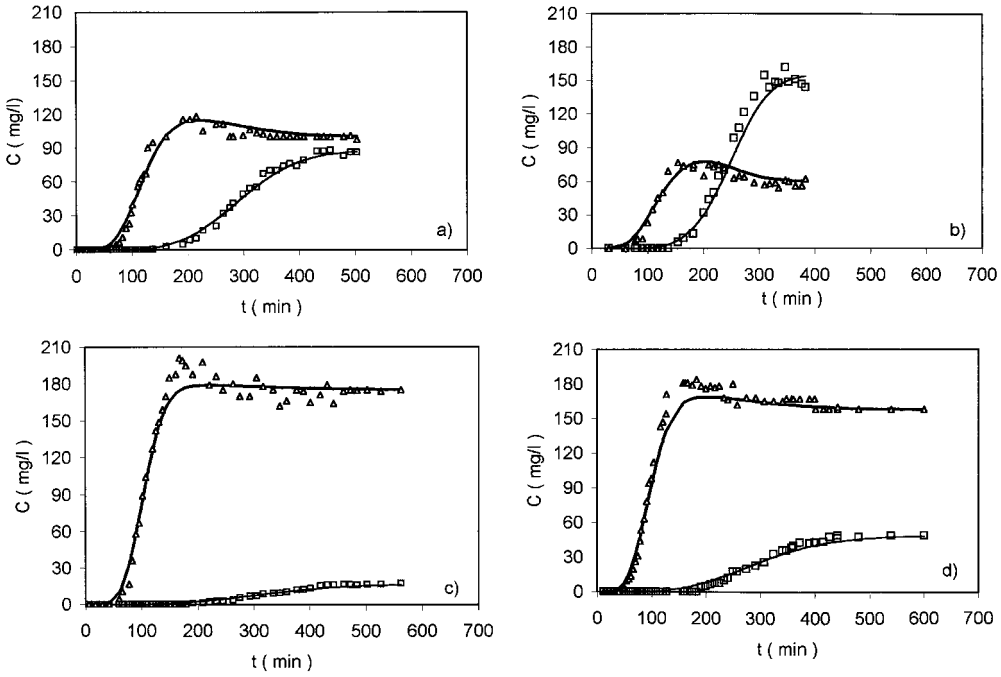

Figure 4. Effect of the feed concentrations on breakthrough curves for binary mixtures of phenol (△△△) and m-cresol (□□□) fed to the column: (a) $C_{f1} = 100$ mg/l, $C_{f2} = 88$ mg/l (run 3); (b) $C_{f1} = 60$ mg/l, $C_{f2} = 156$ mg/l (run 5); (c) $C_{f1} = 175$ mg/l, $C_{f2} = 18$ mg/l (run 9); (d) $C_{f1} = 158$ mg/l, $C_{f2} = 49$ mg/l (run 6).

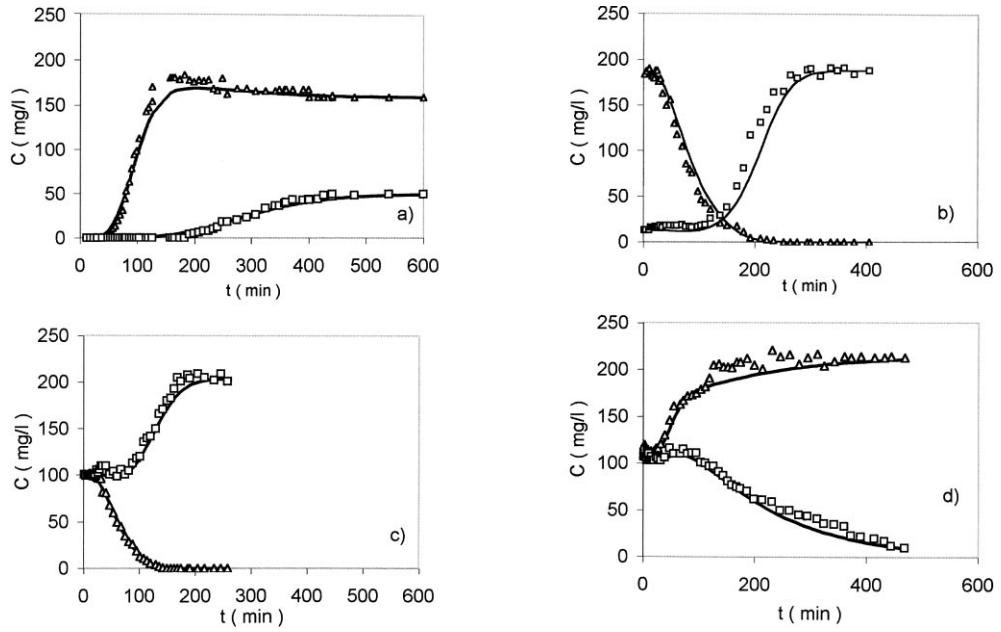

Figure 5. Effect of the bed initial conditions on outlet concentration curves for binary mixtures of phenol (△△△) and m-cresol (□□□) fed to the column: (a) bed initially clean: $C_{01} = C_{01} = 0$; feed composition: $C_{f1} = 158$ mg/l, $C_{f2} = 49$ mg/l (run 6); (b) bed initially pre-saturated: $C_{01} = 185$ mg/l, $C_{02} = 13$ mg/l; feed composition: $C_{f1} = 0$, $C_{f2} = 188$ mg/l (run 13); (c) bed initially pre-saturated: $C_{01} = 100$ mg/l, $C_{02} = 104$ mg/l; feed composition: $C_{f1} = 0$, $C_{f2} = 204$ mg/l (run 11); (d) bed initially pre-saturated: $C_{01} = 108$ mg/l, $C_{02} = 102$ mg/l; feed composition: $C_{f1} = 214$ mg/l, $C_{f2} = 0$ (run 12).

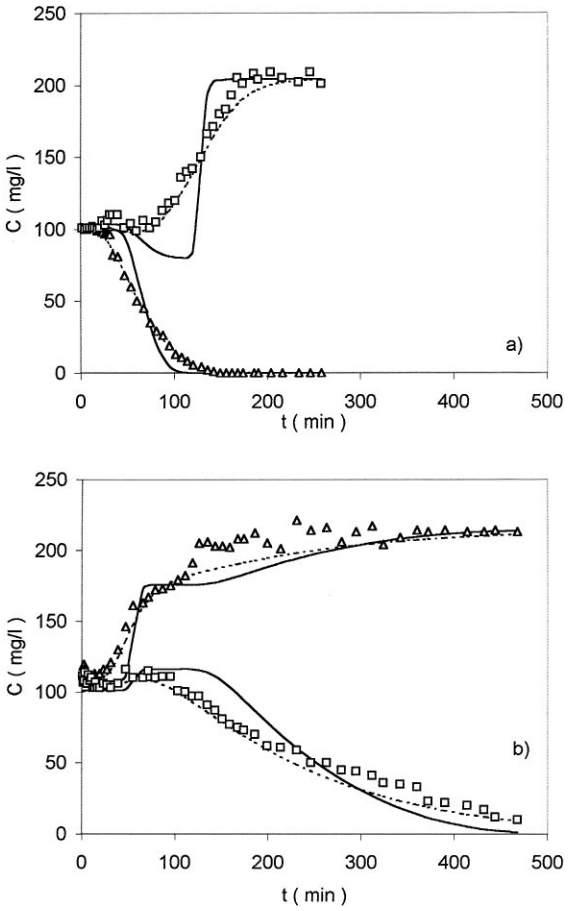

Figure 6. Fixed-bed outlet concentration curves for binary mixtures of phenol (△△△) and m-cresol (□□□): ——equilibrium model; - - - - - pore diffusion model: (a) bed initially pre-saturated: C_{01} = 100 mg/l, C_{02} = 104 mg/l; feed composition: $C_{f1} = 0$, C_{f2} = 204 mg/l (run 11); (b) bed initially pre-saturated: C_{01} = 108 mg/l, $C_{02} = 102$ mg/l; feed composition: $C_{f1} = 214$ mg/l, $C_{f2} = 0$ (run 12).

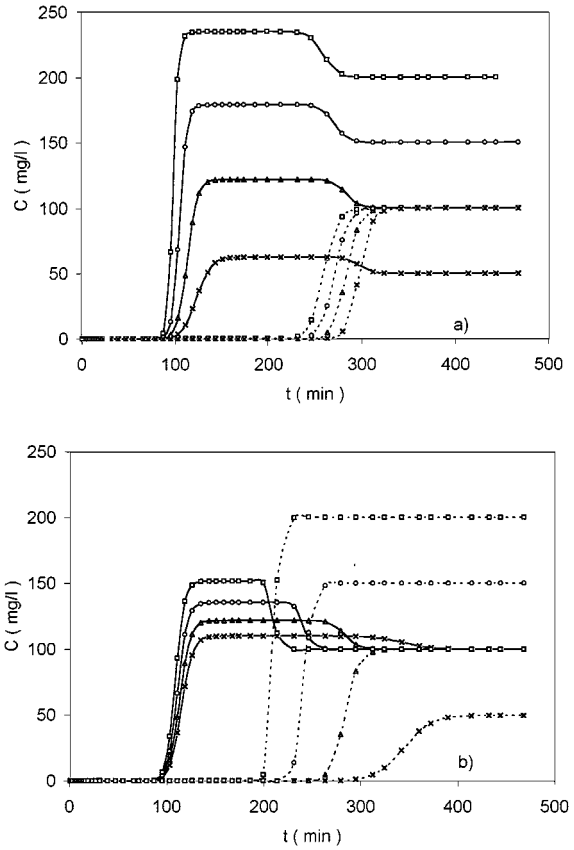

Figure 7. Calculated fixed bed breakthrough curves for binary mixtures of phenol (——) and m-cresol (- - - -): Effect of the feed composition: (a) feed with a constant m-cresol concentration (C_{f2} = 100 mg/l) and different phenol concentrations C_{f1}(mg/l): 200 (□□□); 150 (○○○); 100 (△△△); 50 (×××); (b) feed with a constant phenol concentration (C_{f1} = 100 mg/l) and different m-cresol concentrations: C_{f2} (mg/l): 200 (□□□); 150 (○○○); 100 (△△△); 50 (×××).

phenol in Fig. 6(b) is clearly observed at shorter times in the absence of mass transfer resistances (equilibrium model).

Figure 7 shows the calculated breakthrough curves for a clean bed, when binary mixtures of phenol and m-cresol are fed to the column. In Fig. 7(a) the inlet concentration of m-cresol is taken to be constant ($C_{f2} = 100$), whereas in Fig. 7(b) the inlet concentration of phenol is taken to be constant ($C_{f1} = 100$). As the inlet concentration of phenol increases, in Fig. 7(a), m-cresol is being less adsorbed in agreement with the isotherm equation. As the inlet concentration of m-cresol increases, in Fig. 7(b), phenol is also being less adsorbed. The displacement of phenol by m-cresol is higher as the inlet m-cresol concentration increases, due to the higher affinity of the resin for m-cresol when its concentration increases.

Figure 8 shows the calculated outlet concentration curves for phenol and m-cresol for a pre-saturated bed ($C_{01} = C_{02} = 100$), when only phenol is fed to the column in several concentrations, Fig. 8(a), and when only m-cresol is fed to the column in several concentrations, Fig. 8(b). From these figures, we can observe that the displacement of m-cresol by phenol is enhanced by increasing the feed concentration of phenol, Fig. 8(a), while the displacement of phenol by m-cresol is not affected by the inlet concentration of this component, Fig. 8(b).

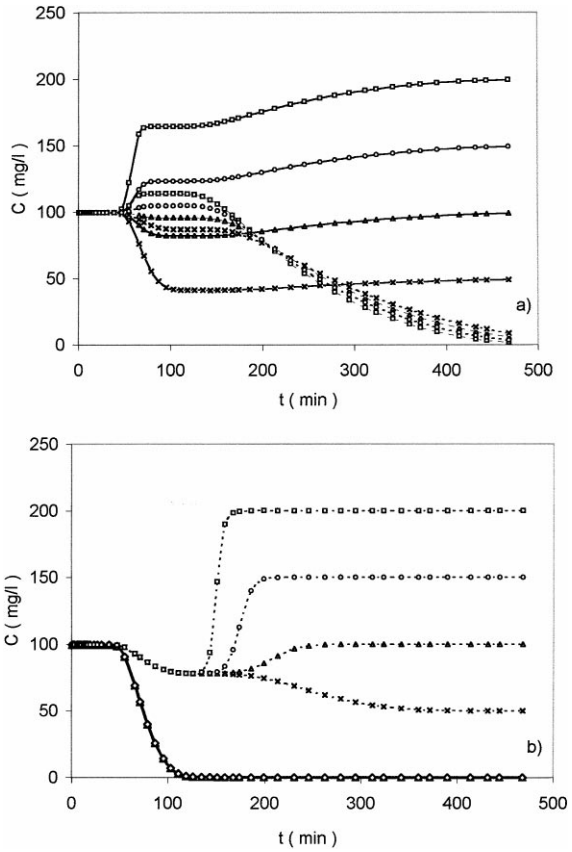

Figure 8. Calculated outlet concentration curves for binary mixtures of phenol (——) and m-cresol (- - - - -) fed to the pre-saturated fixed-bed: (a) feed with a constant m-cresol concentration ($C_{f2} = 0$) and different phenol concentrations C_{f1}(mg/l): 200 (□□□); 150 (○○○); 100 (△△△); 50 (×××); (b) feed with a constant phenol concentration ($C_{f1} = 0$) and different m-cresol concentrations C_{f2}(mg/l): 200 (□□□); 150 (○○○); 100 (△△△); 50 (×××).

6. Conclusions

In this work the binary adsorption of phenol and m-cresol mixtures in a fixed-bed packed with a polymeric adsorbent was studied. Experimental concentration curves of phenol and m-cresol at bed outlet were obtained for different flowrates, feed concentrations and bed initial conditions.

A mathematical model considering dispersed plug-flow for the bulk liquid, external mass transfer resistance, intraparticle mass transfer by pore diffusion and instantaneous equilibrium of adsorption at the pore/wall interface was presented to simulate the fixed-bed adsorption. The equilibrium was predicted by using an extended Langmuir isotherm equation for two components based on single component equilibrium data. The model successfully simulated the adsorption behaviour of the phenol and m-cresol mixtures.

Nomenclature

C	Solute concentration in the bulk liquid phase, mg/l
C_f	Solute concentration in the feed, mg/l
C_p	Solute concentration in the liquid inside particle pores, mg/l
C_0	Liquid phase concentration of solute inside the column at initial time, mg/l
D_{ax}	Bed axial dispersion coefficient, cm^2/s
D_m	Molecular diffusivity, cm^2/s
D_p	Solute effective diffusivity, cm^2/s
d_p	Adsorbent particle diameter, cm
K_L	Langmuir equilibrium constant, l/mg
K_f	Film mass transfer coefficient, cm/s
L	Bed length, cm
N_d	Number of mass transfer units for intraparticle pore diffusion ($=\tau\varepsilon_p D_p/R^2$), dimensionless
N_f	Number of mass transfer units for external film diffusion ($=3\frac{1-\varepsilon}{\varepsilon}\frac{K_f\tau}{R}$), dimensionless
Pe	Bed axial Peclet number ($=u_i L/D_{ax}$), dimensionless
Q_L	Maximum adsorption capacity of the adsorbent, mg/g
q^*	Adsorbed solute concentration in equilibrium with the liquid concentration, mg/g
r	Particle radial coordinate, cm
R	Absorbent particle radius, cm
t	Time, s
u_i	Bed intersticial velocity, cm/s
u_0	Bed superficial velocity, cm/s
u^*	Reduced radial coordinate in the particle ($=r/R$), dimensionless
U	Volumetric flowrate, cm^3/s
X_0	Dimensionless liquid phase concentration of solute inside the column at initial time ($=C_0/C_f$)
X	Dimensionless solute concentration in the bulk liquid phase ($=C/C_f$)
X_p	Dimensionless solute concentration in the liquid inside particle pores ($=C_p/C_f$)
y	Total (liquid + adsorbed) concentration of the solute inside particle pores, mg/l
z	Bed axial coordinate, cm
z^*	Reduced axial coordinate in the bed ($=z/L$), dimensionless

Greek Letters

ε Bed porosity, dimensionless
ε_p Particle porosity, dimensionless
τ Bed space time ($=\varepsilon L/u_0$), s
τ_p Adsorbent tortuosity factor, dimensionless
ρ_a Particle apparent density, g/l
ν Kinematic fluid viscosity

Subscripts

1 Phenol
2 m-Cresol

References

Calleja, G., J. Serna, and J. Rodríguez, "Kinetics of Adsorption of Phenolic Compounds from Wastewater onto Activated Carbon," *Carbon*, **31**, 691–697 (1993).

Costa, C. and A. Rodrigues, "Design of Cyclic Fixed Bed Adsorption Processes I—Phenol Adsorption on Polymeric Adsorbents," *AIChE J.*, **31**, 1645–1654 (1985a).

Costa, C. and A. Rodrigues, "Design of Cyclic Fixed Bed Adsorption Processes II—Regeneration and Cyclic Operations," *AIChE J.*, **31**, 1655–1665 (1985b).

Ferreira, L., "Dinâmica de Processos de Sorção," Ph.D. Thesis, University of Porto, 1994.

Finlayson, B., *Nonlinear Analysis in Chemical Engineering*, McGraw-Hill, 1980.

Garcia, A. and C. King, "The Use of Basic Polymer Sorbents for the Recovery of Acetic Acid from Dilute Aqueous Solution," *Ind. Eng. Chem. Res.*, **28**, 204–212 (1989).

Gruenfeld, M. and U. Frank, *Oil Spill Conference Proceedings*, 487, American Petroleum Institute, Washington, 1997.

Gusler, G., T. Browne, and Y. Cohen, "Sorption of Organics from Aqueous Solution onto Polymeric Resins," *Ind. Eng. Chem. Res.*, **32**, 2727–2735 (1993).

Madsen, N. and R. Sincovec, "PDECOL: General Collocation Software for Partial Differential Equations," *ACM Trans. Math. Software*, **5**, 326–351 (1979).

Mckay, G. and B. Al-Duri, "Prediction of Bisolute Adsorption Isotherms using Single Component Data for Dye Adsorption onto Carbon," *Chem. Eng. Sci.*, **43**, 1133–1142 (1988).

Moon, H., S. Kook, and H. Park, "Adsorption of Phenols onto a Polymeric Sorbent," *Korean J. of Chem. Eng.*, **8**, 168–176 (1991).

Myers, A. and J. Prausnitz, "Thermodynamics of Mixed-Gas Adsorption," *AIChE J.*, **11**, 121–127 (1965).

Reich, R., W. Ziegler, and K. Rogers, "Adsorption of Methane, Ethane, and Ethylene Gases and Their Binary and Ternary Mixtures and Carbon Dioxide on Activated Carbon at 212–301 K and Pressures to 35 Atmospheres," *Ind. Eng. Chem. Proc. Des. Dev.*, **19**, 336–334 (1980).

Ramalho, E., "Adsorção Multicomponente de Fenois," Ph.D. Thesis, University of Porto, 1993.

Rixey, W. and C. King, "Fixed-Bed Multisolute Adsorption Characteristic of Non-wet Adsorbents," *AIChE J.*, **35**, 69–74 (1989).

Suwanayuen, S. and R. Danner, "A Gas Adsorption Isotherm Equation Based on Vacancy Solution Theory," *AIChE J.*, **26**, 68–76 (1980).

Wakao, N. and J. Smith, "Diffusion in Catalyst Pellets," *Chem. Eng. Sci.*, **17**, 825–832 (1962).

Weisz, P. and A. Schwartz, "Diffusivity of Porous-Oxide-Gel-Derived-Catalyst Particles," *J. Catal.*, **1**, 339–404 (1962).